STM JOURNALS

Journal of
Thermal Engineering and Applications

ISSN: 2349-8994
Volume 12, Issue 1, 2025
January–April
DOI (Journal): 10.37591/JoTEA

https://journals.stmjournals.com/jotea

Research | JoTEA

Thermal Performance of Concentrating Solar Panels

Carlos Armenta-Déu*[1], Juan Aguirre[2]

Abstract

The study shows a detailed analysis of the thermal performance of concentrating solar panels and the temperature increase due to concentrated solar radiation. This work proposes a configuration to reduce temperature rise, maintain good panel efficiency, and increase output power. The configuration is based on a sandwich structure including a phase change material (PCM), which absorbs the thermal energy excess generated by the concentrated solar radiation onto the PV panel. The PCM incorporates a heat exchanger consisting of metallic fins that distribute the absorbed heat into the PCM homogeneously, avoiding thermal gradients and the hot point creation. This study examines the effects of weather, materials, and cooling systems on their efficiency. It also covers new cooling methods that help prevent overheating and increase the panels' lifespan. By analyzing both experimental data and computer simulations, this paper provides insights for enhancing CSPs to improve energy output and ensure long-term use. The new configuration shows promising results according to experimental tests for solar radiation above the standard maximum value of 1000 W/m^2. A carried-out modeling process results in adjusting algorithms to the parameters involved in the study, which allows the prediction of PV module performance under variable concentrated solar radiation.

Keywords: Thermal performance, heat exchange, phase change material, solar radiation concentration

INTRODUCTION

Photovoltaic modules currently operate under solar radiation below the maximum standard value on Earth's surface. The PV module temperature increase due to heat generation in the photoelectric conversion reduces the panel efficiency and limits the output power. This effect increases if the PV module operates under concentrated solar radiation because the panel cannot evacuate the heat generation excess.

Many attempts to solve thermal energy evacuation appear in the literature, some inserting heat exchangers [1, 2], others applying thermoelectric converters [3, 4], some others considering underground installations or rapid heat evacuation techniques [5, 6] or using phase change materials [7–9].

Virtually all the works mentioned before regarding conventional PV panel operation under solar radiation equal and below the maximum standard value on Earth's surface, 1 kW/m^2. Nevertheless, in recent times, solar concentration has been used to increase output power in PV arrays, generating a thermal energy surplus that requires an evacuation method to avoid excessive PV panel temperature rise. To this goal, some research develops specific techniques to evacuate the energy excess; among them, we can mention the heat pipes use [10–12], which is the current method to extract thermal energy from the PV panel when overheated due to the increased solar radiation level.

In this work, we develop a new configuration based on the existing PCM sandwich layout with metallic fins incrusted, favoring heat dissipation and

***Author for Correspondence**
Carlos Armenta-Déu
E-mail: cardeu@fis.ucm.es

Faculty, Department of Physical Sciences, Complutense University of Madrid, Madrid, Spain

Received Date: November 25, 2024
Accepted Date: December 11, 2024
Published Date: December 21, 2024

Citation: Carlos Armenta-Déu, Juan Aguirre. Thermal Performance of Concentrating Solar Panels. Journal of Thermal Engineering and Applications. 2025; 12(1): 1–10p.

PV module thermal regulation. The new configuration applies to a PV panel submitted to concentrated solar radiation for a concentration ratio up to 2.1 regarding the standard value on Earth's surface.

Fundamentals

Solar radiation striking the front surface of a photovoltaic panel generates electricity through the photoelectric effect and releases heat due to the thermal losses in the energy conversion process. The heat generation in a PV module depends on the solar radiation level and the module efficiency; mathematically:

$$Q_L = \left(1-\eta_{PV}\right) G S_{PV} t_{op} \tag{1}$$

G is the incoming solar radiation onto the PV panel, in W/m^2, S_{PV} is the PV module front surface, in m^2, t_{op} is the operating time, and η_{PV} is the PV panel efficiency.

If the PV module operates under concentrated solar radiation, Eq. (1) converts into:

$$Q_L = \left(1-\eta_{PV}\right) C_r G S_{PV} t_{op} \tag{2}$$

C_r represents the concentration ratio, defined as:

$$C_r = S_{ap} / S_{PV} \tag{3}$$

S_{ap} accounts for the aperture surface of the concentration device.

Since a PPV module is a non-homogeneous material structure, there is not a single value for the specific heat; therefore, we must determine the equivalent specific heat using the expression:

$$c_{PV}^{eq} = \frac{\sum_{i=1}^{n} m_i c_i}{m_{PV}} \tag{4}$$

m and c represent the mass and specific heat of every PV panel component, i, and m_{PV} is the global mass of the photovoltaic module.

Applying the basic equation for a mass heating:

$$Q_L = m_{PV} c_{PV}^{eq} \Delta T_{PV} \tag{5}$$

ΔT_{PV} is the PV panel temperature increase due to heat losses during the photovoltaic conversion.

For a PV module operating under concentrated solar radiation, we have:

$$\left(1-\eta_{PV}\right) C_r G S_{PV} t_{op} = m_{PV} c_{PV}^{eq} \Delta T_{PV} \tag{6}$$

Operating in Eq. (6):

$$\Delta T_{PV} = \frac{\left(1-\eta_{PV}\right) C_r G S_{PV} t_{op}}{m_{PV} c_{PV}^{eq}} \tag{7}$$

We realize that the linear increase in temperature depends on the operating time, which may lead to an extremely high temperature for a sufficiently long time.

Photovoltaic module temperature evolves with time, increasing its value until it reaches a thermal equilibrium between energy gained from heat generation and thermal radiation to the environment. The equation that defines the thermal balance equilibrium is:

$$m_{PV} c_{PV}^{eq} \Delta T_{PV}^{th} = \sigma \varepsilon_{PV} S_{PV} \left[\left(T_{PV}^{th} \right)^4 - T_{amb}^4 \right] t_{op} \tag{8}$$

Journal of Thermal Engineering and Applications
Volume 12, Issue 1
ISSN: 2349-8994

σ is the Stefan-Boltzmann constant, ε_{PV} is the PV panel emissivity, T_{amb} is the ambient temperature, and $T_{PV}{}^{th}$ is the PV module equilibrium temperature.

Considering the PV panel starts at ambient temperature:

$$m_{PV} c_{PV}^{eq} \left(T_{PV}^{th} - T_{amb}\right) = \sigma \varepsilon_{PV} S_{PV} \left[\left(T_{PV}^{th}\right)^4 - T_{amb}^4\right] t_{op} \tag{9}$$

Developing the term into brackets yields:

$$m_{PV} c_{PV}^{eq} = \sigma \varepsilon_{PV} S_{PV} \left[\left(T_{PV}^{th}\right) + T_{amb}\right]\left[\left(T_{PV}^{th}\right)^2 + T_{amb}^2\right] t_{op} \tag{10}$$

For current operational temperatures, we can use the following approximation:

$$\left[\left(T_{PV}^{th}\right) + T_{amb}\right]\left[\left(T_{PV}^{th}\right)^2 + T_{amb}^2\right] \approx \left(C_r + 0.3\right)\left(T_{PV}^{th}\right)^3 \tag{11}$$

Within 98.7% accuracy.

Combining Eqs. (10) and (11):

$$m_{PV} c_{PV}^{eq} = \left(C_r + 0.3\right) \sigma \varepsilon_{PV} S_{PV} \left(T_{PV}^{th}\right)^3 t_{op} \rightarrow T_{PV}^{th} = \left[\frac{m_{PV} c_{PV}^{eq}}{\left(C_r + 0.3\right) \sigma \varepsilon_{PV} S_{PV} t_{op}}\right]^{1/3} \tag{12}$$

Applying Eq. (6):

$$T_{PV}^{th} = \left[\frac{\left(1 - \eta_{PV}\right) C_r G}{\left(C_r + 0.3\right) \sigma \varepsilon_{PV} \left(T_{PV}^{th} - T_{amb}\right)}\right]^{1/3} \rightarrow T_{PV}^{th} \simeq \left[\frac{\left(1 - \eta_{PV}\right) C_r G}{\left(C_r + 0.3\right) \sigma \varepsilon_{PV} T_{amb}}\right]^{1/3} \tag{13}$$

Eq. (13) provides a practical expression to determine the PV panel temperature at the equilibrium as a function of the concentration ratio, the solar radiation, the panel efficiency and emissivity, and the ambient temperature.

Simulation and Experimental Validation

PV panel thermal analysis: therefore, we simulated variable concentration ratio from a minimum of 0.32 to a maximum of 1.776, comparing the results with data obtained from experimental tests. Figure 1 shows the comparative analysis between theoretical predictions (dashed line) and experimental values (continuous line).

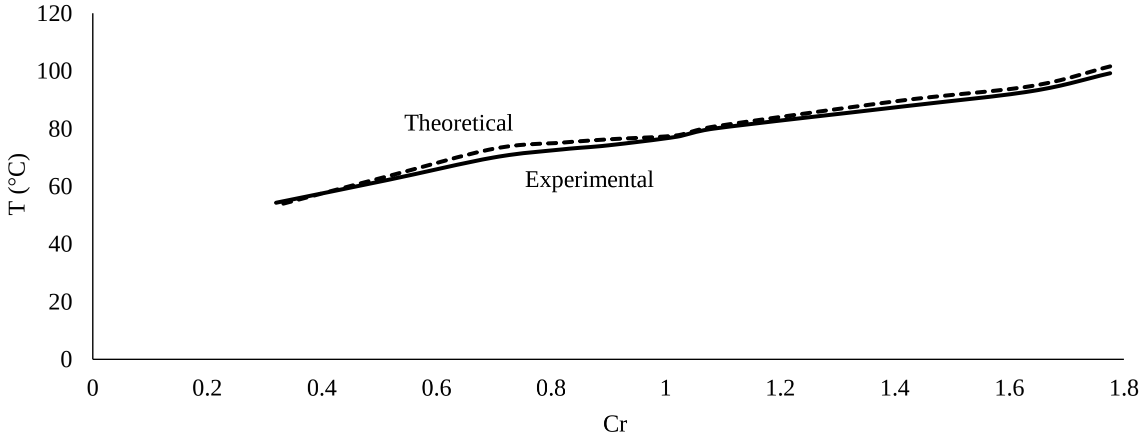

Figure 1. Theoretical and experimental steady state PV panel temperature.

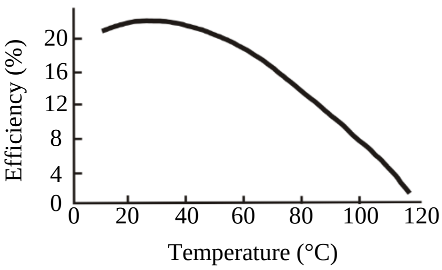

Figure 2. PV module efficiency evolution with temperature.

Table 1. PV module efficiency vs concentration ratio.

	Concentration ratio									
	0.320	0.515	0.700	0.820	0.920	1.020	1.084	1.411	1.639	1.776
η (%)	19.79	18.29	16.39	15.59	15.20	14.37	13.57	11.38	9.86	7.79

We observe a good correlation between theoretical and experimental data with a 1.6 standard deviation and 98.1% accuracy.

THERMAL ENERGY BALANCE

The optimum operational temperature for a PV panel corresponds to the Nominal Operating Cell Temperature (NOCT), 25°C, as shown in Figure 2 [13]. If we compare this optimum value with steady-state temperature under concentrated solar radiation (Figure 1), we notice a PV panel overheating with working temperatures much higher than recommended.

Applying steady state working temperatures to the PV module efficiency evolution, we notice that the performance reduces drastically for all concentration ratios. Table 1 shows the operational efficiency of the PV panel for every concentration ratio.

We observe how the efficiency declines with increasing working temperature, especially for solar radiation concentration. Correlating temperature and efficiency values, we obtain the following dependence:

$$\eta_{PV} = -0.2709T_{PV} + 35.097 \quad (R^2 = 0.994) \tag{14}$$

If we correlate PV panel efficiency and solar radiation concentration, we have:

$$\eta_{PV} = -7.8227C_r + 22.191 \quad (R^2 = 0.994) \tag{15}$$

We should minimize or eliminate the photovoltaic panel temperature increase to recover the optimum efficiency; to do so, we must design a system to evacuate the excess in heat generation by using any of the heat transfer mechanisms, conduction, convection, radiation, or a combination of both. The system consists of a PCM layer (improved paraffin wax) attached to the rear side of the panel with metal fins incrusted to favor heat transfer to the PCM bulk (Figure 3) [14–18].

The PCM heat sink is attached to the PV with no intermediate air layer to improve heat transfer and avoid thermal perturbations. Metal fins distribution makes the heat flow easily reach all the PCM bulk sections. Table 2 shows the PCM layer characteristics. Metal fins are 10 mm thick, 10 mm high, and 200 mm long.

Because of the specific configuration of a PV module, conduction is the most efficient heat transfer mechanism to evacuate the surplus of heat generation. Applying the thermal conduction equation, we have:

$$\dot{Q}_{PV} = m_{PV}c_{PV}\frac{dT_{PV}}{dt} = \frac{\kappa}{d}S\left(T_{PV} - T_o\right) \tag{16}$$

κ is the thermal conductivity of the material to which the heat flows from the PV panel, d is the interphase thickness, S is the contact surface, and T_o is the material temperature at the initial state.

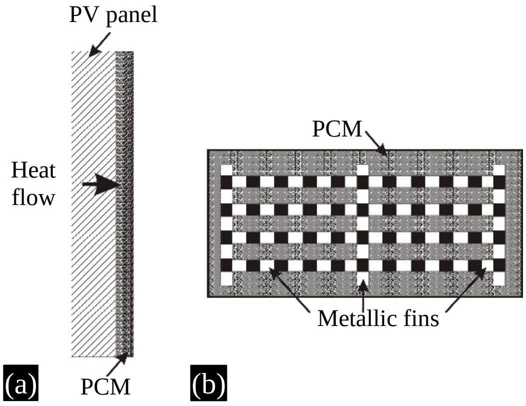

Figure 3. Schematic view of the PV module with attached PCM heat sink. (a) side view and (b) upper view.

Table 2. PCM layer characteristics [19–21].

Characteristic	Value
Density (kg/m^3)	900
Specific heat (J/kg°C)	2.52
Thermal conductivity (W/m.K)	0.267
Latent heat (kJ/kg)	147
Melting point* (°C)	53
Mass (kg)	1.8

(*) The melting point is the average value of the phase change temperature range.

Considering the material temperature remains constant, operating in Eq. (16) yields:

$$T_{PV}^{opt} = T_o + e^{at_c} \tag{17}$$

With:

$$a = \frac{\kappa S}{m_{PV} c_{PV} d} \tag{18}$$

t_c is the time required for the PV module to reach the optimum temperature, T_{PV}^{opt}.

Since any material increases its temperature when collecting heat from an external source, we use a phase change material (PCM), which operates in the solid-to-liquid phase change during the heat removal; therefore, we guarantee a constant temperature operation.

Nevertheless, the PCM starts at ambient temperature, which currently does not match the melting point; in such a case, the thermal energy balance for the PCM is:

$$\frac{1}{t_{ht}}\left[m_{PCM} c_{PCM}\left(T_{PCM}^{mp} - T_{amb}\right) + m_{PCM}^{ml} L_{PCM}\right] = m_{PV} c_{PV} \frac{dT_{PV}}{dt} = \frac{\kappa}{d} S\left(T_{PV} - T_o\right) \tag{19}$$

m_{PCM}, c_{PCM}, and L_{PCM} represent the mass, specific heat, and latent heat of the PCM, T_{PCM}^{mp} is the PCM melting point temperature, and T_{amb} is the ambient temperature, used as the reference value at the starting point of the heat transfer process; m_{PCM}^{ml} is the melted PCM mass and t_{ht} is the heat transfer operating time.

Applying Eq. (19) to the steady state at the end of the heat transfer process and operating, we have:

$$t_{ht} = \frac{d}{\kappa S}\left\{\frac{\left[m_{PCM} c_{PCM}\left(T_{PCM}^{mp} - T_{amb}\right) + m_{PCM} L_{PCM}\right]}{T_{PV} - T_{amb}}\right\} \tag{20}$$

Eq. (20) determines the minimum time for reaching the PV module temperature steady state matching the PCM melting temperature.

Simulation and Experimental Validation

The simulation runs for a hybrid system consisting of a PV panel with a PCM layer attached to the rear side of the panel. Table 3 shows the system characteristics. Paraffin wax thermal conductivity enhances if adding organic material to the bulk [22]. Using data from Figure 1, we obtain the following PV panel temperatures at the initial state (Table 4). Replacing values from Tables 2 and 3 in Eq. (20), yields (Figure 4).

Analyzing results from Figure 1, we observe that the hybrid PV-PCM system requires between 5 and 12 min to reach the final steady-state temperature after heat evacuation; this time is considered acceptable for PV array current operation.

If we correlate the time and solar radiation concentration ratio, we obtain:

$$t_{ht} = 7.1157\left(C_r\right)^{-0.473} \quad (R^2 = 0.9944) \tag{21}$$

Eq. (21) permits determining the required time to stabilize the PV panel temperature after heat removal as a function of the solar radiation concentration ratio.

We developed experimental tests aimed to verify the validity of Eqs. (20) and (21) and data from the simulation. To do so, we submitted the PV panel to variable solar radiation using a solar lamp whose radiation flux varies through a power supply controller. We adjusted the solar radiation flux to match the simulation concentration ratio values. Figure 5 shows the comparative results for theoretical predictions and experimental values.

Table 3. System characteristics.

Characteristic	Value
PV maximum output power (W)	10
PV front surface (m^2)	0.2
PCM mass (kg)	1.8
PCM layer thickness (m)	0.01
Interphase thickness (m)	0.005

Table 4. PV module initial steady-state temperature vs concentration ratio.

	Concentration ratio									
	0.320	0.515	0.700	0.820	0.920	1.020	1.084	1.411	1.639	1.776
T(°C)	54.3	62.2	70.0	72.8	74.2	77.2	80.0	87.6	93.0	99.2

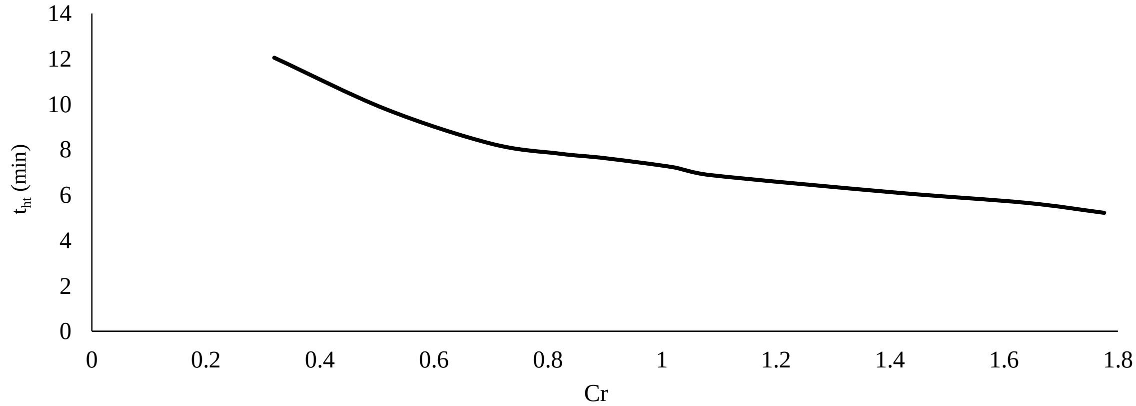

Figure 4. Time to reach PV module final steady-state temperature vs. concentration ratio.

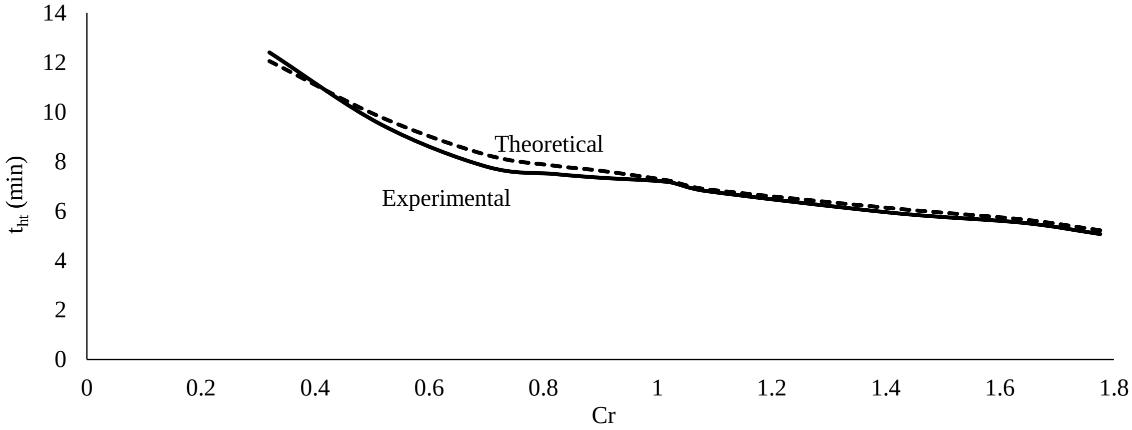

Figure 5. Comparative results between theoretical predictions and experimental values for the time to reach PV module final steady-state temperature vs. concentration ratio.

Table 5. Percentage variation of solar radiation for the heat transfer process interval.

	Concentration ratio									
	0.320	0.515	0.700	0.820	0.920	1.020	1.084	1.411	1.639	1.776
ΔG (%)	0.397	0.609	1.292	1.995	2.462	1.503	1.236	0.933	0.540	0.246

We notice the high correlation between theoretical predictions and experimental values with 97.6% accuracy and 2.23 standard deviation.

PV MODULE THERMAL PERFORMANCE

Despite the short time range for stabilizing the PV panel temperature with heat removal through conduction to the PCM layer, the solar radiation evolves continuously, limiting the applicability of the proposed algorithms.

Solar radiation changes every moment, modifying the concentration ratio and the PV panel temperature. Nevertheless, we may consider the solar radiation time evolution as a series of intervals and determine the solar radiation percentage variation in every interval to evaluate the influence of the heat transfer process time. Table 5 shows the results of the calculation.

We observe that the percentage variation of the solar radiation always remains below 2.5%, with an average value of 1.2%; therefore, we estimate that the solar radiation barely changes during the time the PV panel requires to reach the steady state after heat removal and that the simulation and calculated steady-state PV panel temperatures are valid.

As in the case for the thermal balance, we run a set of experimental tests aimed to demonstrate the validity of the above statement. To this goal, we submitted the PV panel to solar radiation with variable concentration ratio according to preset values, recording temperature evolution with time.

The red lines in Figure 6 show the verification process of the developed simulation. The verification procedure is as follows:

- Temperature evolution is drawn for every concentration ratio (Figure 6).
- Starting at the initial point, we move along the lowest concentration ratio curve for a time if the simulation predicts the PV panel to reach the steady state (point 1).
- We now move backward to meet the next concentration ratio curve at the same PV panel temperature (point 2) to adapt the PV panel temperature evolution to the new concentration ratio according to daily changes in solar radiation after the developed time interval.
- We move again on the second concentration ratio curve for the required time to reach the steady state for this operating condition (point 3).

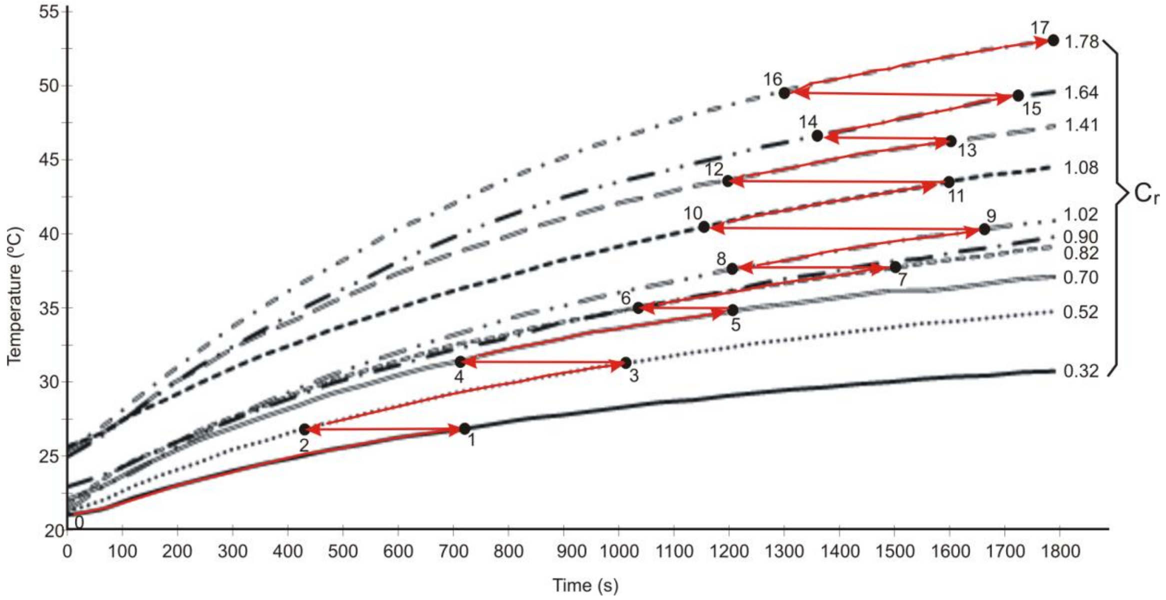

Figure 6. Evaluation of PV panel thermal performance for daily variation of solar radiation.

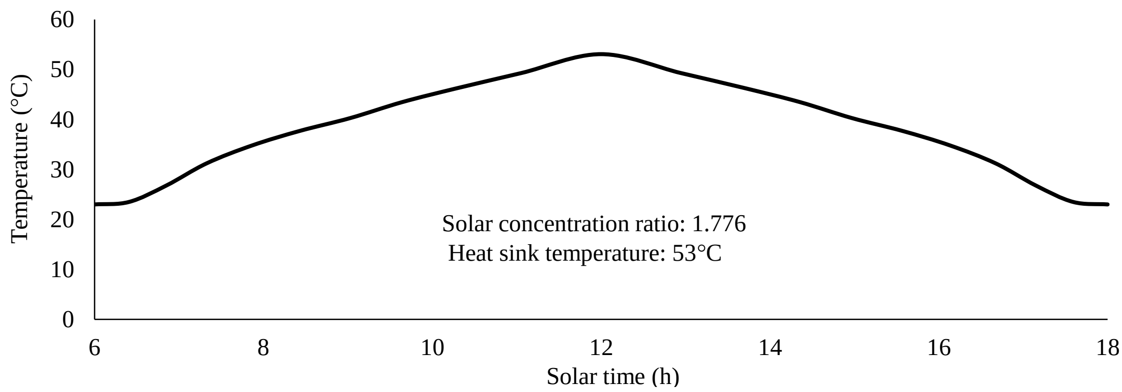

Figure 7. Daily evolution of PV panel temperature submitted to concentrated solar radiation with attached heat sink.

- We repeat the process, moving back and forth from one concentration ratio curve to the next one, applying the simulation time to reach the PV panel temperature steady state in every case.
- The process finishes at point 17 after applying the last simulation time for the highest concentration ratio.

We observe that the procedure leads the temperature panel to 53.1°C, barely 0.1°C above the expected value, demonstrating the validity of the carried-out study. Now, representing the daily time evolution of PV panel temperature for a standard day of 12 solar hours, and considering a midday solar radiation value equivalent to the maximum concentration ratio used in the analysis, we have (Figure 7).

The analysis of Figure 6 shows that the PV panel temperature never exceeds the heat sink steady state temperature when operating in the phase change gap, improving thermal performance and increasing global efficiency. Since in current conditions, with no heat removal, the PV panel may reach a maximum temperature near 100°C.

CONCLUSION

The analysis of PV module thermal performance under concentrated solar radiation shows a significant increase in working temperature, reducing the PV panel efficiency and limiting the output power. A hybrid system consisting of a PCM layer with incrusted metal fins is attached to the rear side of the PV panel with no air interphase. The PCM is a heat sink to collect heat removal from the PV module, maintaining the system operating temperature constant.

Conduction heat transfer is homogeneously distributed in the PCM bulk thanks to the metal fins, compensating the poor thermal conductivity of the PCM material and improving the removal of heat generation surplus in the PV module due to the concentrated solar radiation.

A practical expression to determine the PV panel temperature at the equilibrium as a function of the concentration ratio, the solar radiation, the panel efficiency and emissivity, and the ambient temperature is developed. Theoretical simulation run for solar radiation concentration ratio in the range 0.32 to 1.776 shows that the PCM maintains the PV panel working temperature equal to or below the PCM melting point, 53°C. Experimental tests run under identical conditions to simulation show a high agreement with theoretical predictions with a 1.6 standard deviation and 98.1% accuracy, validating the proposed algorithm.

The developed thermal balance study leads to a mathematical expression of the time the PV panel lasts to reach a steady state in the heat evacuation process. The theoretical expression is correlated to the concentration ratio through a potential function within an accuracy higher than 99%. Experimental tests validate the theoretical predictions, showing a 97.6% accuracy and 2.23 standard deviation.

PV module thermal performance has been evaluated to validate the proposed methodology in determining the PV panel temperature at the steady state for variable solar concentration ratio. The results show that the experimental values match theoretical predictions within 0.1°C.

The present study represents a practical method to determine the steady state operating temperature of PV modules when subjected to concentrated solar radiation, allowing us to estimate the PV panel energy efficiency for every solar radiation level.

REFERENCES

1. Rajvikram M, Sivasankar G. Experimental study conducted for the identification of best heat absorption and dissipation methodology in solar photovoltaic panel. Sol Energy. 2019 Nov 15; 193: 283–92.
2. Kumar R, Montero FJ, Lamba R, Vashishtha M, Upadhyaya S. Thermal management of photovoltaic-thermoelectric generator hybrid system using radiative cooling and heat pipe. Appl Therm Eng. 2023 Jun 5; 227: 120420.
3. Kane A, Verma V, Singh B. Optimization of thermoelectric cooling technology for an active cooling of photovoltaic panel. Renew Sustain Energy Rev. 2017 Aug 1; 75: 1295–305.
4. Armenta-Déu C. Hybrid PV-TEG system to improve performance. International Journal of Microwave Engineering and Technology (IJMET). 2021; 7(2): 26–42.
5. Valiente-Blanco I, Lopez-Pascual D, Diaz-Villar P, Mallol-Poyato R, Barragan A, Ocaña M, Granello G, Diez-Jimenez E. Efficiency improvement of photovoltaic solar modules by cooling using an underground heat exchanger. J Sol Energy Eng. 2022 Dec 1; 144(6): 061015.
6. Akbarzadeh A, Wadowski T. Heat pipe-based cooling systems for photovoltaic cells under concentrated solar radiation. Appl Therm Eng. 1996 Jan 1; 16(1): 81–7.
7. Cui Y, Zhu J, Zhang F, Shao Y, Xue Y. Status and future development of hybrid PV/T system with PCM module: 4E (energy, exergy, economic and environmental) assessments. Renew Sustain Energy Rev. 2022 Apr 1; 158: 112147.
8. Lamba R, Montero FJ, Rehman TU, Singh S, Manikandan S. PCM-based hybrid thermal management system for photovoltaic modules: A comparative analysis. Environ Sci Pollut Res. 2024 Jul; 31(34): 46397–416.

9. Hassan A, Wahab A, Qasim MA, Janjua MM, Ali MA, Ali HM, Jadoon TR, Ali E, Raza A, Javaid N. Thermal management and uniform temperature regulation of photovoltaic modules using hybrid phase change materials-nanofluids system. Renew Energy. 2020 Jan 1; 145: 282–93.
10. Shouquat HM, Abd RN, Selvaraj JA, Pandey AK. Experimental Investigation on Energy Performance of hybrid PV/T-PCM system. In 2019 IEEE 5th International Conference on Electrical Energy Systems (ICEES). 2019 Feb 21; 1–5.
11. Anderson WG, Dussinger PM, Sarraf DB, Tamanna S. Heat pipe cooling of concentrating photovoltaic cells. In 2008 33rd IEEE Photovoltaic Specialists Conference. 2008 May 11; 1–6.
12. Arabkoohsar A, Ismail KA, Machado L, Koury RN. Energy consumption minimization in an innovative hybrid power production station by employing PV and evacuated tube collector solar thermal systems. Renew Energy. 2016 Aug 1; 93: 424–41.
13. Ahmad L, Khordehgah N, Malinauskaite J, Jouhara H. Recent advances and applications of solar photovoltaics and thermal technologies. Energy. 2020 Sep 15; 207: 118254.
14. Luque A, Hegedus S, editors. Handbook of Photovoltaic Science and Engineering. United Kingdom: John Wiley & Sons; 2011.
15. Paul J, Kadirgama K, Samykano M, Pandey AK, Tyagi VV. A comprehensive review on thermophysical properties and solar thermal applications of organic nano composite phase change materials. J Energy Storage. 2022 Jan 1; 45: 103415.
16. Ibrahim SI, Ali AH, Hafidh SA, Chaichan MT, Kazem HA, Ali JM, Isahak WN, Alamiery A. Stability and thermal conductivity of different nano-composite material prepared for thermal energy storage applications. South Afr J Chem Eng. 2022 Mar 1; 39(1): 72–89.
17. Paul J, Kadirgama K, Samykano M, Pandey AK, Tyagi VV. A comprehensive review on thermophysical properties and solar thermal applications of organic nano composite phase change materials. J Energy Storage. 2022 Jan 1; 45: 103415.
18. Qureshi ZA, Ali HM, Khushnood S. Recent advances on thermal conductivity enhancement of phase change materials for energy storage systems: a review. Int J Heat Mass Transfer. 2018 Dec 1; 127: 838–56.
19. Liu L, Su D, Tang Y, Fang G. Thermal conductivity enhancement of phase change materials for thermal energy storage: A review. Renew Sustain Energy Rev. 2016 Sep 1; 62: 305–17.
20. Sigma Aldrich. Paraffin Wax. [Online]. https://www.sigmaaldrich.com/MY/en/product/aldrich/327204
21. Trigui A, Karkri M, Boudaya C, Candau Y, Ibos L. Development and characterization of composite phase change material: thermal conductivity and latent heat thermal energy storage. Compos B: Eng. 2013 Jun 1; 49: 22–35.
22. Freund Mihály, Mózes Gyula. *Paraffin products: properties, technologies, applications*. Translated by Jakab E. Amsterdam, the Netherlands: Elsevier; 1982; 121. ISBN 978-0-444-99712-8.

